Scattering and attenuation characteristics of corn at multiple frequencies and view angles by model simulation and truck-mounted microwave radiometer

ZHANG Zhongjun[1], ZHANG Lixin[2], XU Ying[1], LIU Jiamin[1], SUN Guoqing[3]

1. *School of Information Science and Technology*, *Beijing Normal University*, *Beijing* 100875, *China*;
2. *China State Key Laboratory of Remote Sensing Science*, *Jointly Sponsored by Beijing Normal University and the Institute of Remote Sensing Applications of Chinese Academy of Sciences*, *Beijing* 100875, *China*;
3. *Department of Geography*, *University of Maryland*, *College Park*, *Maryland* 20742, *USA*

Abstract: To remove vegetation effect in soil moisture retrieval by passive microwave technique at lower frequencies, the τ-ω model is often used. In order to evaluate the scattering and attenuation characteristics of vegetation at higher frequencies, a Matrix-Doubling microwave emission model based on ray-tracing technique was used on corn, to study its single scattering albedo and transmissivity with different height at C (6.925GHz), X (10.65GHz) and Ku (18.7GHz) bands. The comparison between simulation results and the data collected by a truck-mounted microwave radiometer in a field experiment are good. To verify the simulated emission from corn layer only, the ground surface of corn field was placed with an Aluminum foil, so as to mask the emission from the soil. A Brightness Temperature database was setup by assigning a variety of parameters to the verified model, to simulate Brightness Temperature of natural corn field with different height. The results by the Matrix-Doubling model were then matched with those by *τ*-*ω* model at the same condition by least-square deviation, so as to retrieve the effective single scattering albedo and transmissivity of corn at C, X and Ku-band.

Key words: Matrix-Doubling, microwave emission, single scattering albedo, *τ*-*ω* model

CLC number: TP79/TP732.1 **Document code:** A

Citation format: Zhang Z J, Zhang L X, Xu Y, Liu J M and Sun G Q. 2010. Scattering and attenuation characteristics of corn at multiple frequencies and view angles by model simulation and truck-mounted microwave radiometer. *Journal of Remote Sensing*. **14**(2): 396—408

1 INTRODUCTION

Soil moisture is a key parameter of energy exchange that links the surface and atmosphere, and plays an important role in agriculture and forecast. Any improvements in soil moisture retrieval accuracy on a regional or global basis are very important for global water and energy cycling.

Over the past two decades, by passive microwave technique, many field experiments data have been acquired under various conditions with microwave sensors, which led to *τ*-*ω* model (Jackson & Schmugge, 1991), a semi-empirical form of radiative transfer theory. The total Brightness Temperature is represented as:

$$T = T_c(1-\omega)(1-e^{-\tau}) + T_c(1-\omega)(1-e^{-\tau})\gamma_s e^{-\tau} + (1-\gamma_s)T_s e^{-\tau} \quad (1)$$

where ω is single scattering albedo of vegetation, τ is its opacity, and γ_s is surface reflectivity. T_c and T_s are brightness temperature of vegetation and surface, respectively, which are typically treated as the same. Under C band ω usually ranges from 0.05 to 0.15, and τ is defined by vegetation water content, view angle and vegetation species.

In *τ*-*ω* model vegetation is treated as a uniform layer, and multiple scattering effect are ignored. It works well for grasslands, agricultural crops, and light to moderate vegetation under C-band. Currently, both the NASA's AMSR-E (launched in 2002) and Chinese FY-3 (launched in 2008) missions rely on *τ*-*ω* model to retrieve soil moisture. The lowest frequency channel of these sensors is 6.925GHz and 10.65GHz, respectively. When processing data obtained at frequencies higher than C-band, values of ω and τ are still used which are derived at lower frequencies. Recently, a re-examination of some field data sets has shown some evidence of discrepancies between results obtained with a physics-based discrete modeling approach and those obtained with semi-empirical algorithms (Lang *et al.*, 2004). A variety of vegetation species on earth means the complexity of vegetation effect—diversities of both ω and τ at different frequency and view angle (zenith), whose accuracies are important to Brightness Temperature (Adriaan *et al.*, 2004). Multiple scattering effects inside vegetation should

Received: 2009-03-05; **Accepted**: 2009-05-11

Foundation: National Science Fund of China (No.40571108) and National 973 Project of China (No. 2007CB714403).

First author biography: Zhang Zhongjun (1968—), male, Ph.D., Associate Professor. He is currently involved in several projects such as National 973, National Natural Science Found, etc. He has published more than 10 papers. E-mail: zzj@bnu.edu.cn

be considered as frequency goes higher than C-band (Eni *et al.,* 2003). The scattering and penetrating properties of vegetation are largely unknown, which constitute a major gap in our knowledge base.

In this paper, a Matrix-Doubling (thereafter M-D) model is used to simulate microwave emission of corn at C (6.925GHz), X (10.65GHz) and Ku (18.7GHz) bands. Total emission and vegetation layer emission term are verified by a truck-mounted microwave radiometer in a field experiment, respectively. Since M-D model is very complicated, it is difficult to relate the soil emission (soil moisture) directly to Brightness Temperature, while τ-ω model is simple in formula, which is usually used under C-band. In order to elevate accuracy of soil moisture retrieval when processing satellite data at higher frequencies by τ-ω model, we setup a Brightness Temperature database by the M-D model. The results from M-D model are matched with those from τ-ω model at the same conditions by least-square deviation, so as to retrieve effective single scattering albedo and transmissivity of corn at these frequencies.

2 THEORY AND MODEL

The M-D model used in this paper is based on ray-tracing technique, which could account for multiple scattering inside vegetation layer, as well as that between vegetation and soil surface (Ferrazzoli & Guerriero, 1996; Ulaby *et al.*, 1986). When frequency goes higher than C-band, multiple scattering could not be ignored. In this model, vegetation layer is divided into N sub-layers which are assumed to be symmetrical in azimuth, as shown in Fig. 1. At each sub-layer, incident and scattering angle is divided into several intervals, i.e. 5 ° , so that every direction inside vegetation layer could be accounted as much as possible. The smaller the interval (means the more scattering directions inside vegetation layer), the longer the computing time it takes. At one incidence, scattering matrix S and transmission matrix T at nearby sub-layer $\Delta\tau_1$ and $\Delta\tau_2$ could be written as:

$$S = S_1 + T_1^* S_2 T_1 + T_1^* S_2 S_1^* S_2 T_1 + \cdots$$
$$= S_1 + T_1^* S_2 (1 - S_1^* S_2)^{-1} T_1 \quad (2a)$$
$$T = T_2[1 + S_1^* S_2 + (S_1^* S_2)^2 + \cdots] T_1$$
$$= T_2 (1 - S_1^* S_2)^{-1} T_1 \quad (2b)$$

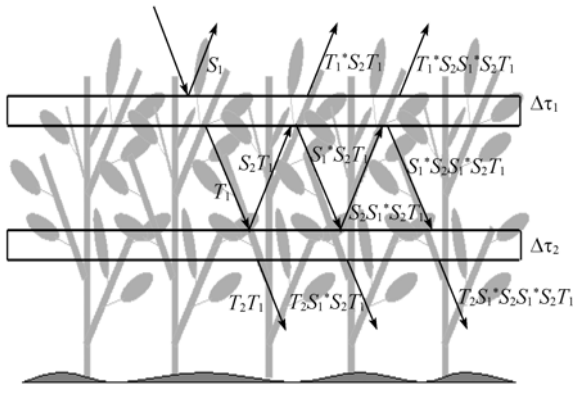

Fig. 1 Matrix-Doubling algorithm

In Eq. (2), S_1 and S_2 represent scattering matrix (incidence from upward, scattering upward) of sub-layer 1 and 2, respectively. T_1 and T_2 represent transmission matrix (incidence from upward, scattering downward) of sub-layer 1 and 2, respectively. The symbols with * represent incidence from downward. The details can be seen in Ulaby *et al.*(1986). Scattering and Transmission matrix of sub-layer (i.e.S_1,T_1 in Eq. (2)) can be calculated by treating its vegetation elements such as leaves, stems, branches or trunks as dielectric discs or cylinders. The details can be found in Karam & Fung(1988). Next, combine sub-layer $\Delta\tau_1$ and $\Delta\tau_2$ into a new but thicker sub-layer $\Delta\tau$, and repeat this calculation and combination N times, besides considering vegetation boundary condition, the total microwave scattering of vegetated surface could be obtained. According to the law of conservation of energy, one minus scattering contribution is emission (Ferrazzoli & Guerriero, 1996).

When Physical Optics model is used on the scattering of corn leaf, its long and curving shape can be considered as several discs with random orientation distribution by the same area (Fig. 2) (Vine *et al.,* 1983). Although Andrea *et al.* proposed a scattering model for curved leaf by treating the leaf as a part of sphere—this looks more like a natural leaf (Della *et al.*, 2004), it involves lots of mathematical integration and costs too much calculating time, so we did not use this model in this paper. For vertical stem of corn, Infinite Length Approximation is used (Karam & Fung, 1988).

Fig. 2 Corn leaf is treated as assemblage of disc with random orientation

The ground model used in M-D model is IEM (Fung, 1994). To overcome the errors when IEM run at higher frequencies and/or large surface roughness, some mathematical techniques were used to avoid overflow, so as to enlarge the parameter range of IEM. At 6.925GHz, 10.65GHz and 18.7GHz, the upper limit of root mean square(RMS)error height could reach to about 2.0cm when volumetric soil moisture was less than 40%. Although AIEM is reported to work well at larger surface roughness and higher frequency (Chen *et al.*, 2003), it is too

complicated in modeling and costs too much computing time, especially in establishing a simulation database, so it was not accepted in our work.

For a corn field with full coverage, the total microwave emission simulated by M-D model is composed of three terms as follows (Ulaby *et al.*, 1986):

(1) Corn layer upward emission——term T_1

(2) Soil upward emission attenuated by corn layer——term T_2

(3) Corn layer emission interaction with soil surface——term T_3

Microwave emission represented by Brightness Temperature T could also be described by emissivity, the equation can be seen in Ulaby *et al.*(1986). At 6.925GHz and V polarization, the simulated emissivity of a corn field of 80cm height, corn layer emissivity (T_1 term), and soil emissivity after passing through corn layer (T_2 term), are shown in Fig. 3, respectively, where we can see that, as view angle increasing, contribution of corn layer increase, soil emission decrease, while the total emissivity keeps almost unchangeable. Also we can see the polarization difference of anyone of the terms is not obvious due to multiple scattering effects, which is quite different from the case at L-band (Karam *et al.*, 1992).

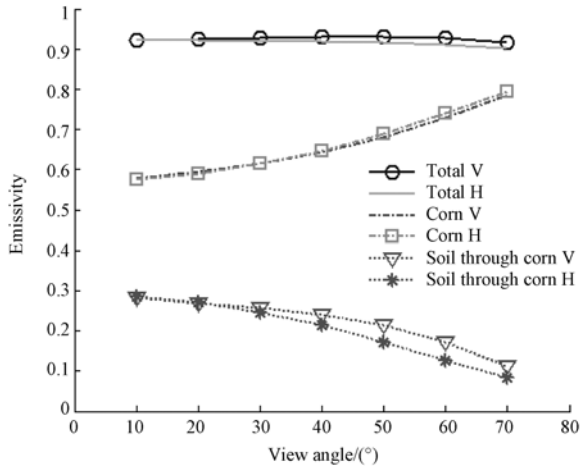

Fig. 3 Emissivity component of corn field at 6.925GHz
(RMS height is 1cm, volumetric soil moisture is 17%, correlation length is 10cm.)

3 MICROWAVE RADIOMETER AND FIELD EXPERIMENT

To verify the microwave emission as well as its terms by M-D model, we did a field experiment at Qing Yuan, Hebei Province of China (N 38°44'53", E 115°28'10") in July 7, 2008, when corn grew to about 80cm. The truck-mounted microwave radiometer we used are made in Germany and owned by the State Key Laboratory of Remote Sensing Science at Beijing, China. It has four frequencies: 6.925GHz, 10.65GHz, 18.7GHz and 36.5GHz, each with dual polarization channel. It is fixed on a motor-driven elevator inside the tank of the truck (Fig. 4). The latter part of the tank is a working room.

The Brightness Temperature range of the radiometer is 0—350 K, the RMS of the radiometric resolution is less than 0.15K. The accuracy is 1.0 K, and stability is less than 0.05K. More characteristics can be seen by visiting http://www. radiometer-physics.com. The weather at that day was good and we used Sky tipping (Tip curve calibration) as the calibration method. It is suitable for those frequencies where the earth's atmosphere opacity is low, which means that the observed sky Brightness Temperature is only influenced by the cosmic background radiation temperature.

Fig. 4 Corn field experiment by microwave radiometer in July 7 at Qing Yuan, Hebei Province, China

During the experiment, the sensor of the radiometer was elevated to about 8 m above the ground. The view angles were set to 50º—60º, because (1) this range is within Chinese FY-3A sensor's viewing scope; (2) signatures at smaller angles less than this were probably affected by metal of the truck, and the corn nearby the road side were not as uniform as inner part; (3) larger view angles would result in larger illuminated area, which would have brought in considerable physical work.

The illuminated area of the radiometer is elliptical, varying a little bit at each frequency. At one frequency, according to the height and view angle of the radiometer, we went to the edge of illuminated site by estimation, and began to move an Aluminum foil (Fig. 4), watching the responsed Brightness Temperature of the radiometer, so as to decide the exact position of the 4 corners of the rectangular where the elliptical illuminated area was embedded. Before receiving radiometry data, geometry parameters of corn, together with soil and environmental parame-

Table 1 Corn parameters

Canopy parameters		Stalk parameters	
Canopy height/cm	83.2	Length/cm	29.3
Plant density/m^{-2}	10	Diameter/cm	2.0
		Density/m^{-2}	10
Leaf length/cm	54.1	Gravimetric moisture/%	60
Leaf width/cm	5.65	Inclination angle	Uniform within ±5°
Leaf thickness/mm	0.29		
Density/plant	7		
Gravimetric moisture/%	65		

ters, were collected as listed in Table 1. Since one cycle of receiving the radiometry data needed less than 10 min, the temperature of vegetation, surface 0—1cm of soil, and environment could be considered as constant while the radiometer was working. The temperature of that day was 34.3ºC, measured by a JM624u thermometer (accuracy is 0.1°C). The gravimetric soil moisture was 17.4%, which was obtained by the weight before and after drying 20 min. The soil surface looked flat and the RMS height was assumed to be 1.0 cm, the correlation length to be 10cm. Also the water content of vegetation samples were obtained by drying in oven. At view angle between 50º and 60º, with the interval of 2.5º, the measured Brightness Temperature at C, X and Ku-band are listed in Table 2, where we can see the data at V pol is larger than H pol by each frequency. This is the final results of the ground emission passing through the corn gap mixed by corn layer emission.

4 SIMULATION AND ANALYSIS

4.1 Emission terms validation

In model simulation, one corn leaf was changed to several random discs with same thickness by the same area. In Table 1, the leaf area was about 306 cm^2, which equals to about 12.2 random discs with radius of 2.85cm (half of width). At 6.925GHz, the simulated total Brightness Temperature by M-D model from view angels between 30º to 70º vs. measured data between 50º and 60º are shown in Fig. 5. Note that since the corn height was lower at early July, there existed many gaps between individual plants, which mean soil emission signatures without any block could be received directly by the radiometer. According to our estimation of the field, the corn coverage was about 80%, and the gap occupied about 20%. This ration is reflected in Fig. 5 where the total emission shown id composed of both corn field and bare soil contribution.

Table 2 Measured Brightness Temperature of corn field

/K

Frequency/GHz	H polarization					V polarization				
	50°	52.5°	55°	57.5°	60°	50°	52.5°	55°	57.5°	60°
6.925	262.35	261.28	258.84	256.00	253.63	272.62	273.88	273.94	273.83	273.83
10.65	263.57	262.18	261.11	261.30	261.77	274.39	275.03	275.41	276.02	276.44
18.7	259.51	259.26	259.03	259.58	260.33	277.40	278.38	279.34	280.37	281.05

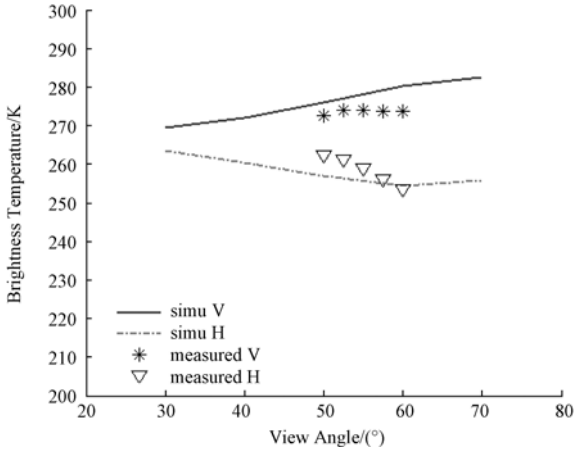

Fig. 5 Comparison of simulation and measured Brightness Temperature at 6.925GHz (80% cover)

Fig. 6 An aluminum foil was placed on the ground under the corn to mask the soil emission

To verify the emission contribution from corn layer only (T_1 term) by M-D model, an aluminum foil was placed on the ground below the corn, so as to mask the soil emission, as shown in Fig. 6. Similar method was used 25 years ago by D. R. Brunfelt. The difference is they based on τ-ω model to derive single scattering albedo of crop by the conclusion that whether to place Aluminum foil or not, total microwave emission come from crop only at middle grow season.

Theoretically the reflectivity of aluminum foil is 1.0, and emissivity is 0. Actually due to the holes in aluminum foil for the corn to grow, and unsmooth of the foil, the reflectivity of aluminum foil could not reach to 1.0. At C-band it was measured as 0.95, and kept almost the same at X- and Ku-band. In M-D model, the soil emissivity was replaced by 1.0 minus reflectivity of aluminum foil, instead of the modified IEM. The simulated Brightness Temperature of corn layer only, after multiplied by 80%, is listed in Table 3(a). The atmosphere emission measured at that day was about 6K. Temperature was 34.3°C. The emissivity of aluminum foil was 0.05. This means besides the radiometry from corn layer only, the sensor received 6K×0.95×20% and 307.3K×0.05×20%, total 4.21K of emission contribution. When view angle vary from 50º to 60º, the measured Brightness Temperature at C, X and Ku band is listed in Table 3(b). The comparison of measured data vs. simulation is good (Fig. 7), where we can find confidence of emission of corn layer only (T_1 term).

4.2 Estimation of corn emission and attenuation

The 0th-order τ-ω model is usually suitable under C-band, vegetation is treated as an uniform layer and does not account

Table 3(a) 80% of simulated Brightness Temperature of corn layer only when ground covered by aluminum foil

/K

Frequency/ GHz	H polarization			V polarization		
	50°	55°	60°	50°	55°	60°
6.925	189.0	193.3	196.7	184.1	185.6	185.6
10.65	204.1	207.4	210.2	204.4	206.2	206.8
18.7	215.1	216.7	218.2	220.6	222.8	224.0

Table 3(b) Measured Brightness Temperature of corn field with aluminum foil cover on ground

/K

Frequency/ GHz	H polarization			V polarization		
	50°	55°	60°	50°	55°	60°
6.925	196.9	190.6	192.7	193.7	189.2	192.5
10.65	195.6	192.5	206.4	195.5	191.4	206.5
18.7	209.7	215.3	221.5	214.9	221.8	229.7

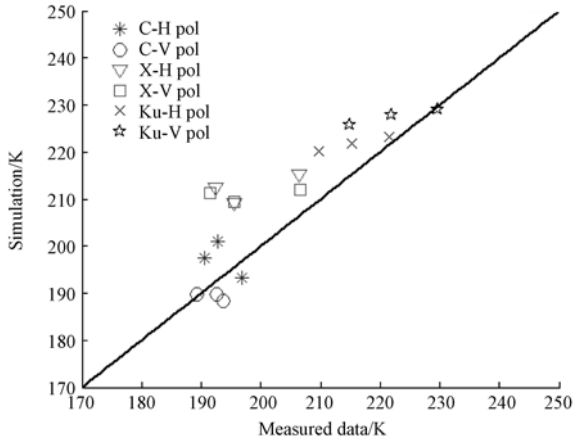

Fig. 7 Comparison of measured data vs. simulation of corn (T_1 term) when ground covered by Aluminum foil

for multiple scattering. The advantage of τ-ω model lies in its simplicity, which could relate the measured data directly to the dielectric constant of surface, hence the soil moisture. It is widely used in explaining data in field experiments such as SMEX, and satellite data such as AMSR-E. Since parameters ω and τ in τ-ω model are obtained in lower frequencies, their behaviors (scattering and attenuation) at higher frequency are unknown. The accuracies are important to soil moisture retrieval.

Since M-D model are very complicated, it is difficult to relate soil moisture to microwave emissivity directly. Based on Eq. (3), we matched the total emission from M-D model with the results from τ-ω model at the same conditions by least-square error, so as to get the effective scattering and attenuation characteristics of vegetation at higher frequencies (Ferrazzoli *et al.*, 2002):

$$\sigma = \sqrt{\sum_{1}^{N}(e_{i1} - e_{i2})^2} \tag{3}$$

where e_{i1} and e_{i2} is emission from M-D model and τ-ω model, respectively. N is the number of simulation.

To simulate all possible cases of natural situation of corn field to get e_{i1} in Eq. (3), a wider range of parameters were assigned to M-D model, such as frequencies, RMS heights and correlation lengths, soil moistures, etc.(Table 4), so as to establish a simulation database of Brightness Temperature. By matching Eq. (1) and (3) we can get the effective single scattering albedo and transmissivity of corn.

Results of corn with different heights at X-band are shown in Fig. 8. Only one polarization is presented, due to no obvious polarization difference were found. Results at three frequencies are listed in Table 5, more results could be found on (Zhang *et al.*, 2008).

Table 4 Parameter Range of M-D model

Frequency / GHz	RMS height / cm	Soil Moisture / %	Correlation length / cm
6.925	0.8—2.0, step=0.2	5—40, step=5	10.0—20.0, Step=5
10.65	0.8—2.0, step=0.2	5—40, step=5	10.0—20.0, Step=5
18.70	0.8—2.0, step=0.2	5—40, step=5	10.0—20.0, Step=5

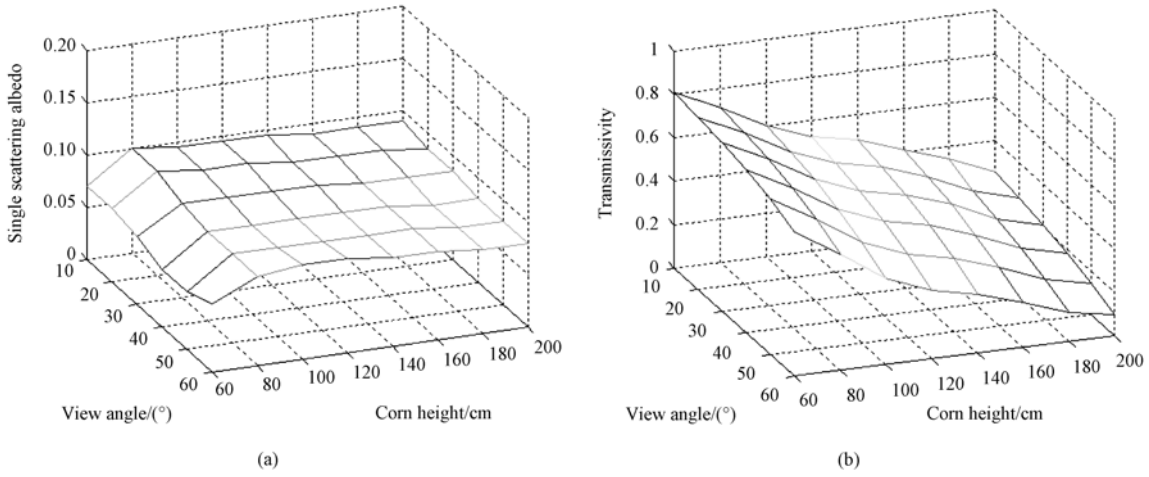

Fig. 8 (a) Effective single scattering albedo of corn at X-band and V pol. vs. view angle and height; (b) Transmissivity of corn at X-band and H pol. vs. view angle and height

Table 5(a) Effective single scattering albedo of corn at V pol (50° view angle)

Height/cm / Frequency/GHz	60	80	100	120	140	160	180	200
6.925	0.025	0.060	0.065	0.070	0.070	0.070	0.070	0.070
10.65	0.055	0.085	0.085	0.085	0.085	0.085	0.080	0.080
18.7	0.085	0.100	0.095	0.095	0.09	0.085	0.085	0.080

Table 5(b) Transmissivity of corn at V pol (50° view angle)

Height/cm / Frequency/GHz	60	80	100	120	140	160	180	200
6.925	0.81	0.71	0.61	0.53	0.46	0.42	0.33	0.28
10.65	0.75	0.64	0.51	0.43	0.39	0.31	0.22	0.18
18.7	0.69	0.56	0.42	0.33	0.25	0.19	0.14	0.10

Unlike τ-ω model, M-D model considers multiple scattering effect. The retrieval results by Eq. (3) are called effective value, with the purpose to extend τ-ω model up to high frequency data. For corn height of 83.2cm, the retrieved effective single scattering albedo and transmissivity at 6.925GHz, V pol and 50° view angle are 0.06 and 0.70, respectively.

5 CONCLUSION AND DISCUSSION

By analyzing the retrieval data of corn at 6.925GHz, 10.65GHz and 18.7GHz on Table 5 and Zhang *et al.* (2008), we can find that:

(1) At any of the frequencies, no obvious polarization differences were found for both ω and τ of corn. This is due to the multiple scattering effect increase as frequency goes high, which decreases polarization effects.

(2) At the same corn height, ω keeps almost the same at these three frequencies. At any of the frequencies, ω varies slightly as corn height increase.

(3) At the same corn height, the higher the frequency, the smaller the transmissivity. Before mid-term the transmissivity of corn ranges between 0.4 and 0.7. If soil moisture were retrieved by satellite data at these frequencies, the soil emission could be considered to be totally masked by corn at the height of 180cm, 160cm and 120cm, corresponding to C, X and Ku band.

The results in this paper would be further verified by satellite data.

Acknowledgements: The authors would give thanks to Dr. Yang Hu and Dr. Wu Shengli, both from China Meteorological Administration, and PhD student Zhao Shaojie from Beijing Normal University, who participated in the experiment. The authors would give special thanks for the anonymous reviewers of this paper.

REFERENCES

Adriaan A, Van G and Wigneron J P. 2004. The b-factor as function of frequency and canopy type at H-polarization. *IEEE Transactions on Geoscience and Remote Sensing*, **42**(4): 786—794

Brunfelt D R and Ulaby F T. 1984. Measured microwave emission and scattering in vegetation canopies. *IEEE Transactions on Geoscience and Remote Sensing*, **22**(6): 520—524

Chen K S, Wu T D and Tsang L. 2003. Emission of rough surfaces calculated by the integral equation method with comparison to three-dimensional moment method simulations. *IEEE Trans actions on Geoscience and Remote Sensing*, **41**(1): 90—101

Fung A K. 1994. Mircrowave Scattering and Emission Models and Their Applications. Norwood, MA: Artech House

Ferrazzoli P and Guerriero L. 1996. Passive microwave remote sensing of forests: a model investigation. *IEEE Transactions on Geoscience and Remote Sensing*, **34**: 433—443

Ferrazzoli P, Guerriero L and Wigneron J P. 2002. Simulating L-band emission of forests in view of future satellite applications. *IEEE Transactions on Geoscience and Remote Sensing*, **40**(12): 2700—2708

Jackson T J and Schmugge T J. 1991. Vegetation effects on the microwave emission from soils. *Remote Sensing of Environment*, **36**: 203—210

Karam M and Fung A K. 1988. Electromegnatic wave scattering from some vegetation samples. *IEEE Transactions on Geoscience and Remote Sensing*, **26**(6): 799—808

Karam M. 1997. A physical model for microwave radiometry of vegetation. *IEEE Transactions on Geoscience and Remote Sensing*, **35**(4): 1045—1058

Lang R, Utku C and O'Neill P. 2004. Role of albedo in assessing soil moisture under vegetation with passive L-band algorithms. Proc. of IGARSS'04 . Anchorage, Alaska, USA

Le Vine D M, Meneghini R and Lang R H. 1983. Scattering from arbitrarily orientated dielectric disks in the physical optics regime. *Journal of the Optical Society of America*, **73**: 1255—1262

Njoku E G, and Jackson T G. 2003. Soil moisture retrieval from AMSR-E. *IEEE Transactions on Geoscience and Remote Sensing*, **41**(2): 215—229

RPG-8CH-DP user manual, Radiometer Physics GmbH Co. http://www.radiometer-physics.com.. (2008-11-25)

Ulaby F T, Moore R K and Fung A K. 1986. Microwave Remote Sensing: Active and Passive,Vol.3. Dedham, MA: Artech House

Vecchia A D, Ferrazzoli P and Guerriero L. 2004. Modeling microwave scattering from long curved leaves. *Waves in Random Media*, **14**(2): S333—S343(1)

Zhang Z J, Zhang L X and Zhao S J. 2008. The technical report of microwave scattering and attenuation characteristics of typical crop. Beijing: Beijing Normal University

用模型和车载微波辐射仪研究多频率多角度下玉米的散射和衰减特性

张钟军[1]，张立新[2]，许　瑛[1]，刘嘉敏[1]，孙国清[3]

1. 北京师范大学 信息科学与技术学院，北京 100875;
2. 遥感科学国家重点实验室，北京师范大学，北京 100875;
3. 马里兰大学 地理系，美国 马里兰州 College Park 20742

摘　要：在使用被动微波技术反演土壤水分的过程中，为去除植被的影响，通常采用适用于低频的 τ-ω 模型。为准确评估较高频率下植被的散射和衰减特性，以玉米为例，采用基于光线跟踪原理的双矩阵(Matrix-Doubling)微波辐射模型，研究不同高度的作物在 C(6.925 GHz)、X(10.65 GHz)和 Ku(18.7 GHz)波段下的单散射反照率和传输率。模型模拟的亮度温度跟车载微波辐射仪的野外实测数据接近。为验证模拟的玉米自身微波辐射，在玉米地上铺设了一层铝箔屏蔽地表的辐射。通过给验证后的模型输入不同的参数，建立一个亮度温度数据库，以模拟自然状态下不同高度玉米的亮度温度。然后把模型模拟的结果，跟相同环境下 τ-ω 模型得到的结果按最小二乘法进行匹配，从而获得不同高度的玉米在 C、X 和 Ku 波段上等效的单散射反照率和传输率。

关键词：双矩阵，微波辐射，单散射反照率，τ-ω 模型

中图分类号：TP79/TP732.1　　文献标识码：A

引用格式：张钟军，张立新，许瑛，刘嘉敏，孙国清．2010．用模型和车载微波辐射仪研究多频率多角度下玉米的散射和衰减特性.遥感学报，**14**(2)：396—408

Zhang Z J, Zhang L X, Xu Y, Liu J M and Sun G Q. 2010. Scattering and attenuation characteristics of corn at multiple frequencies and view angles by model simulation and truck-mounted microwave radiometer. *Journal of Remote Sensing*. **14**(2): 396—408

1　引　言

土壤水分是连接地表和大气层之间能源交换的一个重要参数，它在农业和气象方面起着举足轻重的作用。提高局部或全球范围上的土壤水分反演精度，对地球上水和能量的循环很重要。

在过去的 20 年里，通过被动微波遥感技术和各种微波传感器，获取了许多不同条件下的实验数据，并由此产生了零阶的 τ-ω 模型(Jackson & Schmugge, 1991).该模型是基于辐射传输理论的一种半经验模型，总的亮度温度 T 表示为:

$$T = T_c(1-\omega)(1-e^{-\tau}) + T_c(1-\omega)(1-e^{-\tau})\gamma_s e^{-\tau} + (1-\gamma_s)T_s e^{-\tau} \quad (1)$$

式(1)中 ω 表示植被的单散射反照率，τ 表示植被的光学厚度，γ_s 表示地表的反射率，T_c 和 T_s 分别表示植被和地表的亮温，可以认为相同。C 波段以下 ω 的范围一般在 0.05—0.15，参数 τ 由植被的含水量、观察角度和植被种类等参数确定(Adriaan 等, 2004)。

在 τ-ω 模型中植被看作是均匀介质，多次散射效应被忽略。在低于 C 波段的条件下，它广泛应用于草地、农作物和疏密度不高的植被区域。目前美国宇航局的 AMSR-E(2002 年)、中国的风云 3 号(2008 年)，主要依靠 τ-ω 模型实现土壤水分的反演。这两种传感器的最低频段分别是 6.925 GHz 和 10.65 GHz。处理这些较高频率的卫星数据，植被层 ω 和 τ 的数值仍然沿用低频下推导出来的结果。最近对一些试验数据的研究发现，通过基于物理的离散模型方法获得的结果，跟通过半经验算法获得的结果存在着差异(Lang 等, 2004)。地表上植被类型复杂，在不同频率和观察角度(指天顶角，下同)下的 ω 和 τ 差异很大，其准确性对地表亮温的影响很大(Adriaan 等, 2004)。C 波段以上，植被内部的多次散射效应增

收稿日期：2009-03-05；修订日期：2009-05-11

基金项目：国家自然科学基金项目（编号：40571108）和国家 973 项目第三课题（编号：2007CB714403）。

第一作者简介：张钟军(1968—　)男，博士，副教授，研究方向为微波遥感、信号处理。主持或参加多项国家自然科学基金、国家 973 等科研项目，发表论文十余篇。E-mail: zzj@bnu.edu.cn。

强(Njoku 等, 2003), 植被的微波散射和穿透性有待深入认识和研究。

以玉米为例, 使用双矩阵(Matrix-Doubling, 以下简称 M-D)模型模拟玉米在 C (6.925 GHz)、X (10.65 GHz)和 Ku(18.7 GHz)波段上的微波辐射, 通过车载微波辐射仪进行野外实验, 验证模拟的总微波辐射及其分量。由于 M-D 模型很复杂, 不易把土壤的发射率(土壤水分)跟亮度温度建立直接联系; 而 τ-ω 模型形式上直观, 但一般用于 C 波段以下。因此为把 τ-ω 模型应用到高频率的卫星数据上, 提高反演土壤水分的精度, 我们用 M-D 模型建立了一个亮度温度数据库, 并将 M-D 模型模拟的结果和相同环境下 τ-ω 模型的结果, 按照最小二乘法进行匹配, 从而反演出玉米在 C、X 和 Ku 波段上等效的单散射反照率和传输率。

2 理论和模型

本文中使用的 M-D 模型根据光线跟踪原理, 可以充分考虑植被层内部, 以及植被和地表之间的多次散射(Ulaby 等, 1986; Ferrazzoli & Guerriero, 1996)。当频率高于 C 波段时, 多次散射效果不能忽略。在 M-D 模型中, 植被层被分为 N 个薄子层, 并假设这些子层在方位角上是对称的, 如图 1。对于每一个子层, 入射角和散射角被分成若干间隔, 例如 5°一个间隔。间隔越小, 则越能将植被层内部的每个方向考虑到, 但计算量也越大。对于某个入射方向, 相邻薄子层 $\Delta\tau_1$ 和 $\Delta\tau_2$ 的散射矩阵 S、传输矩阵 T 可以写为(Ulaby 等, 1986):

$$\begin{aligned} S &= S_1 + T_1^* S_2 T_1 + T_1^* S_2 S_1^* S_2 T_1 + \cdots \\ &= S_1 + T_1^* S_2 (1 - S_1^* S_2)^{-1} T_1 \end{aligned} \tag{2a}$$

$$\begin{aligned} T &= T_2[1 + S_1^* S_2 + (S_1^* S_2)^2 + \cdots] T_1 \\ &= T_2 (1 - S_1^* S_2)^{-1} T_1 \end{aligned} \tag{2b}$$

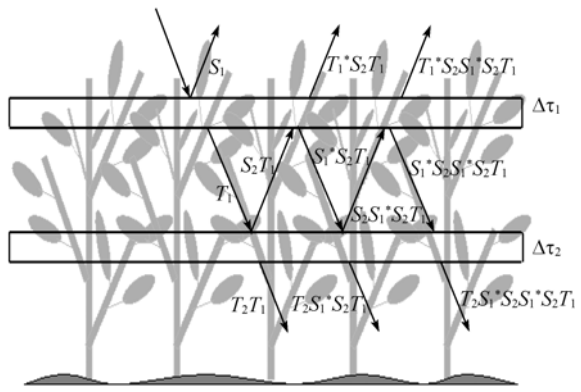

图 1 双矩阵算法

式(2)中 S_1、S_2 分别表示从上面入射时子层 1、2 向上的散射矩阵; T_1、T_2 分别表示子层 1、2 向下的传输矩阵; 而带*号的符号表示从下向上的入射, 详细的解释和定义见 Ulaby 等 (1986)。子层(如式(2)中的 S_1 和 T_1)中植被的叶、茎、枝、主干等散射体看成是具有一定朝向的介电圆片或者介电圆柱体, 其散射和传输矩阵的计算方法见 Karam & Fung, (1988)。将子层$\Delta\tau_1$ 和$\Delta\tau_2$ 组合为一个新的、较厚的子层$\Delta\tau$, 再重复 N 次这种计算和组合, 加上边界条件就可以获得包含地表在内的微波散射。根据能量守恒原理, 1 减去散射即可得到微波辐射(Ferrazzoli & Guerriero, 1996)。

当使用物理光学(Physical-Optics)模型计算玉米叶片的散射时, 弯曲的长玉米叶按总面积折合成若干随机分布的介电圆片(Le Vine 等, 1983), 如图 2。虽然有一种弯曲叶片微波散射模型, 把玉米叶片看成是球体的一部分来近似成自然形状的叶子(Vecchia 等, 2004), 但因为它涉及了太多的数学积分, 计算时间太长, 我们没有采用这种方法。对于玉米杆, 采用了无限长近似(Infinite Length Approximation)理论来计算其散射(Karam & Fung, 1988)。

M-D 模型中的地表部分采用了积分方程模型 IEM(Fung, 1994)。IEM 在高频、大粗糙度下运行容易溢出。在模拟过程中, 为扩大 IEM 的适用范围, 使用一些数学技巧减少溢出。对于本文的频率, 当土壤水分少于 40%时, 均方根高度(rms)的上限值可达到 2 cm。虽然 AIEM 模型适用性更好(Chen 等, 2003), 但是由于它太复杂而且耗费很多的计算时间, 尤其是在建立模拟数据库上, 因而没有采用。

对于覆盖率为 100%的玉米地, 采用 M-D 模型

图 2 玉米叶看成随机朝向的圆盘集合

模拟输出的总微波辐射可以看做 3 部分贡献组成(Ulaby 等, 1986):

(1) 玉米层自身向上的微波辐射 T_1

(2) 地表向上经过玉米衰减后的辐射 T_2

(3) 玉米和地表之间相互作用项 T_3

用亮度温度 T 表示的微波辐射贡献也可以用发射率 e 来描述, 相关公式见 Ulaby 等(1986)。在 6.925 GHz 时模拟的 80 cm 高的玉米总发射率、玉米自身的发射率(T_1 项), 和地表经过玉米衰减后的发射率(T_2 项)如图 3。我们看到随着观察角的增加, 玉米的辐射贡献增大, 地表经过衰减后的发射率减小, 而总的发射率几乎保持不变。同时看到对于同一种辐射来说极化差非常小。这是由于高频下多次散射作用增强, 去极化作用增加的结果。这跟 L 波段下极化差别大的特点不同(Karam, 1997)。

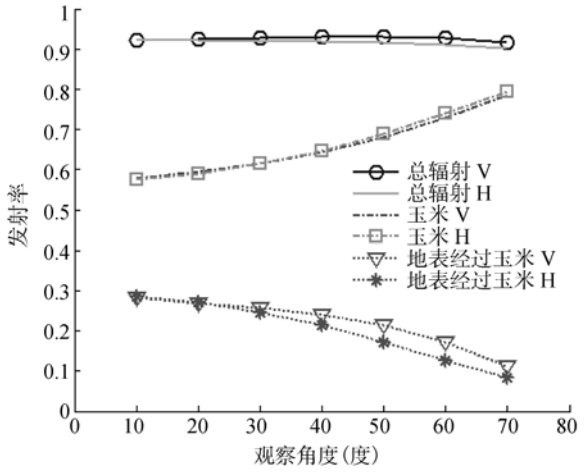

图 3 玉米在 6.925 GHz 的总发射率及其各组成部分
(其中 rms 为 1 cm, 土壤水分为 17%, 相关长度为 10 cm)

3 微波辐射仪和实验

为了验证 M-D 模型模拟的总微波辐射及其分量, 我们于 2008-07-07 在河北省清苑县(北纬 38°44′53″, 东经 115°28′10″)进行了一次玉米实验, 当时玉米大约 80cm 高。实验中使用的车载微波辐射仪由德国 RPG 公司制造, 属于“遥感科学国家重点实验室”。该仪器有 4 个频率: 6.925 GHz, 10.65 GHz, 18.7 GHz 和 36.5 GHz, 每个频率是双极化方式。辐射仪探头固定在卡车车厢内的一个升降台上(图 4), 由液压系统操控升降。车厢后部是工作间。

辐射仪的亮度温度测量范围为 0—350K, 最小的积分时间为 1.0 s, 辐射仪分辨率 rms 小于 0.15K, 绝对亮度温度的准确度为 1.0K, 热稳定度小于 0.05K,

图 4 2008-07-07 在河北清苑用微波辐射仪观测玉米的实验

具体指标见(http://www.radiometer-physics.com)。实验当天的气象状况理想, 采用了天空校准(sky tipping)作为校准方法。这种方法适用于观察到的大气光学厚度较低的频率, 也就是说可观测的天空亮度温度仅受宇宙背景辐射温度的影响。

实验过程中辐射仪的探头升至离地面高大约 8m。观察角度范围设置为 50º—60º, 这是因为(1)这个范围位于中国风云 3 号(FY-3A)微波成像仪的视角范围内; (2)太小的角度, 信号有可能受到卡车金属外壳和田边树林的影响, 而且靠近田边的玉米长势并不如里边的均匀; (3)较大的观察角度会导致对应像元面积增大, 实验的工作量也增大。

辐射仪的照射区域呈椭圆形, 随不同频率略有变化。对于某一频率, 先根据辐射仪的准确高度和观察角度, 粗略地估计出照射范围, 然后走到边缘处开始移动铝箔(图 4), 同时观察辐射仪的亮度温度反应, 从而确定出椭圆所在矩形的 4 个角的准确位置。在开始接收微波辐射数据的之前, 测出玉米的几何参数、土壤和环境参数, 见表 1。一个亮温测量周期为 10min 左右, 可以认为植被温度、地表 0—1cm 的温度、环境温度等相同且保持不变。用 JM624u 铂金电阻温度计(精度是 0.1℃)实测的温度为 34.3℃。为测土壤重量含水量, 用采样后称重、烘干 20min 后再称重的方法, 测得的结果为 17.4%。土壤表面很平, rms 高度假定为 1.0 cm, 相关长度为 10 cm。植被的含水量也是采用称重后烘干的方法测量的。观察角度在 50º—60º, 间隔为 2.5°时, C、X 和 Ku 波段上所测得的亮度温度列于表 2。可以看出相同频率下, V 极化的亮温要高于 H 极化, 这是由于玉米空隙透出的裸露地表辐射, 以及玉米自身辐射的共同作用结果。

4 模拟和分析

4.1 辐射项验证

模拟过程中，如前所述，玉米叶看成若干等厚度随机朝向的介电圆片。由表 1 的实测参数可知，一片叶子的面积大约是 306 cm^2，相当于 12.2 个半径为 2.85 cm(宽度的一半)的随机圆片。频率为 6.925 GHz 时，模拟的总亮度温度跟实测数据的对比如图 5。其中模拟的观察角度范围为 30º—70º，实测数据范围为 50º—60º(表 2)。需要说明的是，由于 7 月初玉米高度仍然较低，单株作物之间存在许多空隙，这就意味着部分地表辐射信号可以无任何阻挡地直接被辐射仪接收。根据估计，实验期间玉米的覆盖率大约是 80%，空隙率大约为 20%(图 5)，即模拟的总微波辐射是由玉米和裸土的贡献共同组成。

表 1 玉米参数

作物参数		杆参数	
高度/cm	83.2	杆参数长度/cm	29.3
株密度/m^{-2}	10	直径/cm	2.0
叶参数长度/cm	54.1	密度/m^{-2}	10
宽度/cm	5.65	含水量/%	60
厚度/mm	0.29	倾角	±5°均匀分布
密度/株	7		
含水量/%	65		

表 2 实测玉米的亮度温度

/K

频率/GHz	H 极化					V 极化				
	50°	52.5°	55°	57.5°	60°	50°	52.5°	55°	57.5°	60°
6.925	262.35	261.28	258.84	256.00	253.63	272.62	273.88	273.94	273.83	273.83
10.65	263.57	262.18	261.11	261.30	261.77	274.39	275.03	275.41	276.02	276.44
18.7	259.51	259.26	259.03	259.58	260.33	277.40	278.38	279.34	280.37	281.05

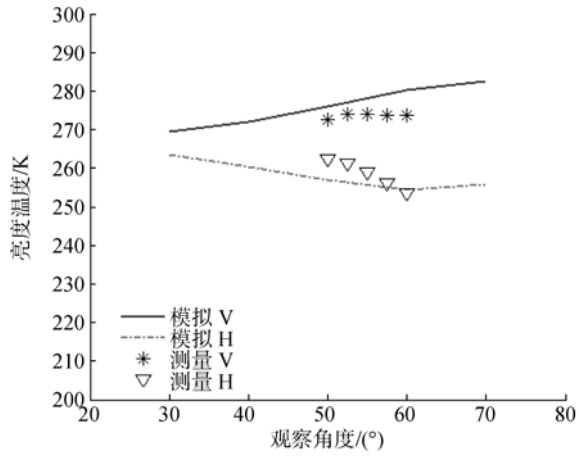

图 5 频率为 6.925 GHz 时模拟和实测的亮度温度比较(玉米)

为研究玉米自身的辐射贡献，即 M-D 模型输出的 T_1 项，在玉米下边的地表上铺设了一层铝箔来屏蔽地表的微波辐射，见图 6。这种做法借鉴了 25 年前 Brunfelt 等(1984)的做法。所不同的是，他们的依据是 τ-ω 模型，根据生长中期的作物总辐射仅来自植被层，是否铺设铝不会影响亮温的结论，推导出低频下的单散射反照率。

图 6 在玉米下面覆盖铝箔，来屏蔽地表微波辐射

理论上铝箔的反射率为 1.0，发射率为 0。实际上由于铺设的铝箔要给作物生长留出缝隙，铝箔本身有褶皱、起伏等因素，使得铝箔的反射率达不到理论值。C 波段实测的铝箔反射率是 0.95，且在 X 和 Ku 波段上基本保持不变。在 M-D 模型里面，我们用 1.0 减去铝箔的反射率替换由 IEM 给出的地表发射率。模拟出的玉米亮度温度乘以 80%的覆盖率后列在表 3(a)中。当天所测得的大气辐射大约为 6 K，测量时环境温度为 34.3ºC，铝箔自身的发射率为

0.05，这就意味着微波辐射仪除了玉米自身的微波辐射外，又接收了 6K×0.95×20%以及 307.3K×0.05×20%共 4.21 K 的辐射贡献。当观察角度为 50º—60º 时，由 C、X 和 Ku 波段测出的亮度温度如表 3(b)。模拟和实测数据的对比结果见图 7，可以看出两者很相近，说明模型输出的玉米自身辐射(T_1 分量)是可靠的。

表 3 (a) 铺设铝箔后模拟的玉米自身亮度温度的 **80%** /K

频率/GHz	H 极化			V 极化		
	50°	55°	60°	50°	55°	60°
6.925	189.0	193.3	196.7	184.1	185.6	185.6
10.650	204.1	207.4	210.2	204.4	206.2	206.8
18.700	215.1	216.7	218.2	220.6	222.8	224.0

表 3(b) 铺设铝箔的玉米地实测的亮度温度 /K

频率/GHz	H 极化			V 极化		
	50°	55°	60°	50°	55°	60°
6.925	196.9	190.6	192.7	193.7	189.2	192.5
10.650	195.6	192.5	206.4	195.5	191.4	206.5
18.700	209.7	215.3	221.5	214.9	221.8	229.7

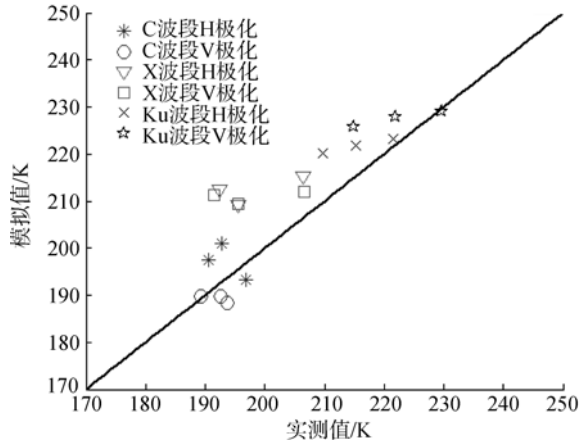

图 7 地表覆盖铝箔时玉米的实测数据跟模拟数据对比(T_1 项)

4.2 玉米的辐射和衰减特性估计

零阶的 τ-ω 模型通常适用于 C 波段下，植被层看成均匀介质，忽略多次散射效果。该模型的优势在于它的简单性，可以将实测的亮温数据跟地表的发射率，进一步说就是土壤水分，直接联系在一起，因此广泛应用于 SMEX 系列的实验、AMSR-E 的卫星数据等。由于 τ-ω 模型中的参数 ω 和 τ 在低频下得到(Jackson & Schmugge, 1991; Adriaan 等, 2004)，在高频下植被的散射和衰减特性是否仍可以沿用低频结果却是未知的。其准确性对提高较高频率下被动微波遥感数据反演土壤水分的精度很重要。

由于 M-D 模型非常复杂，难于把土壤水分和微波发射率直接建立联系。我们按照(3)式，把 M-D 模型所得到的结果，跟相同环境下的 τ-ω模型得到的结果，用最小二乘法进行匹配，从而得到 C、X 和 Ku 波段下玉米的等效散射和衰减特性(Ferrazzoli 等, 2002):

$$\sigma = \sqrt{\sum_{1}^{N}(e_{i1} - e_{i2})^2} \tag{3}$$

式(3)中 e_{i1} 和 e_{i2} 分别是 M-D 模型和 τ-ω 模型的发射率，N 是总的模拟次数。

为了模拟自然状态下的各种玉米，获取式(3)中 e_{i1}，按不同的频率给 M-D 模型假设了一个较大范围的输入参数，如最小均方根 (rms) 高度、相关长度、土壤水分等(表 4)，从而建立了一个亮度温度的模拟数据库。然后通过式(1)、(3)，反演出玉米的等效单散射反照率和传输率。

表 4 M-D 模型模拟的参数范围

频率/GHz	均方根高度 /cm	土壤水分/%	相关长度 /cm
6.925	0.8—2.0, 步长 0.2	5—40, 步长 5	10.0—20.0, 步长 5
10.650	0.8—2.0, 步长 0.2	5—40, 步长 5	10.0—20.0, 步长 5
18.700	0.8—2.0, 步长 0.2	5—40, 步长 5	10.0—20.0, 步长 5

不同高度的玉米 X 波段下的结果如图 8。由于没有发现很明显的极化差异，图 8 只给出了一种极化结果。玉米 3 种频率的结果列在表 5 中(V 极化)，更多的结果参见 Zhang 等(2008)。

跟 τ-ω 模型不同的是，M-D 模型考虑了多次散射效果，因此用式(3)反演出的单散射反照率称之为等效值，目的是把 τ-ω 模型拓展到高频数据上。对于高度为 83.2cm 的玉米地，玉米完全覆盖，在 6.925GHz、V 极化和 50°观察角度时，反演的等效单散射反照率和传输率分别为 0.06 和 0.70。

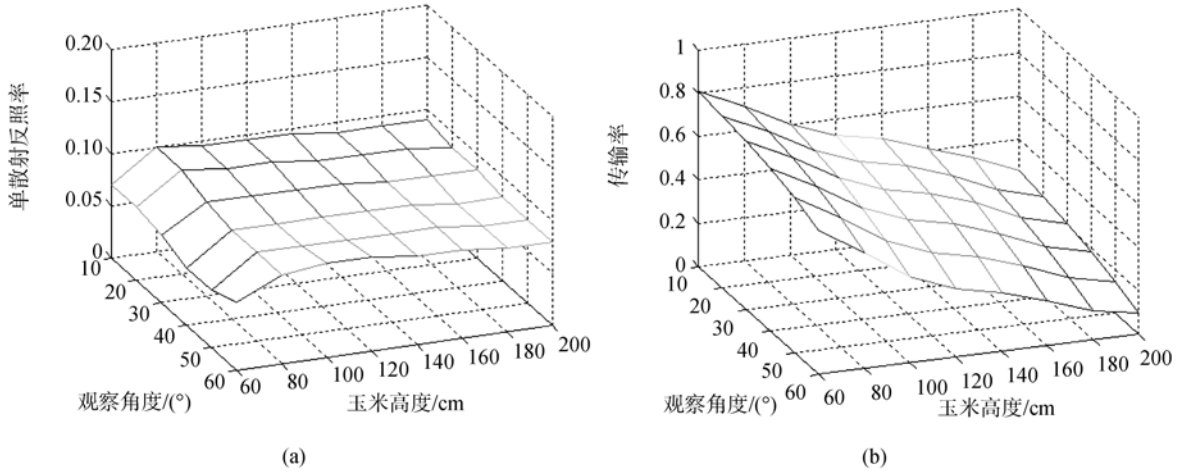

图 8 (a)玉米 X 波段 V 极化的等效单散射反照率跟观察角度和作物高度的关系; (b)玉米 X 波段 H 极化的传输率跟观察角度和作物高度的关系

表 **5(a)** 玉米 **V** 极化的等效单散射反照率(50°观察角)

高度/cm / 频率/GHz	60	80	100	120	140	160	180	200
6.925	0.025	0.060	0.065	0.070	0.070	0.070	0.070	0.070
10.65	0.055	0.085	0.085	0.085	0.085	0.085	0.080	0.080
18.7	0.085	0.100	0.095	0.095	0.09	0.085	0.085	0.080

表 **5(b)** 玉米 **V** 极化的传输率(50°观察角)

高度/cm / 频率/GHz	60	80	100	120	140	160	180	200
6.925	0.81	0.71	0.61	0.53	0.46	0.42	0.33	0.28
10.65	0.75	0.64	0.51	0.43	0.39	0.31	0.22	0.18
18.7	0.69	0.56	0.42	0.33	0.25	0.19	0.14	0.10

5 结论和讨论

通过分析玉米在 6.925 GHz、10.65 GHz 和 18.7 GHz 波段上反演的数据见表 5 和 Zhang 等(2008), 可以得出一些初步的结论。

(1) 任何一种频率下玉米的 ω 和 τ 参数没有明显的极化差别。这是由于较高频率下多次散射增强, 削弱了极化的影响。

(2) 在 3 种频率下高度相同的玉米 ω 数值差别不大。相同频率下 ω 随着玉米高度的增加而略有差异。

(3) 高度相同的玉米, 频率越高传输率越小。玉米生长到中期之前, 3 种频率下的传输率大约在 0.4—0.7。若用这 3 种频率的卫星数据反演中后期玉米地的土壤水分, 可以认为地表的微波辐射在 3 种频率下完全被玉米屏蔽的高度依次为 180, 160, 120cm。

本文的结果将在应用于卫星数据过程中加以检验和完善。

致 谢 感谢中国气象局卫星中心的杨虎副研究员、武胜利博士, 以及北京师范大学地理与遥感科学学院的赵少杰等研究生共同参与了实验。同时也感谢本文匿名审阅者提出的宝贵修改意见。

REFERENCES

Adriaan A, Van G and Wigneron J P. 2004. The b-factor as function of frequency and canopy type at H-polarization. *IEEE Transactions on Geoscience and Remote Sensing*, **42**(4): 786—794

Brunfelt D R and Ulaby F T. 1984. Measured microwave emission and scattering in vegetation canopies. *IEEE Transactions on Geoscience and Remote Sensing*, **22**(6): 520—524

Chen K S, Wu T D and Tsang L. 2003. Emission of rough surfaces calculated by the integral equation method with comparison to three-dimensional moment method simulations. *IEEE Transactions on Geoscience and Remote Sensing*, **41**(1): 90—101

Fung A K. 1994. Mircrowave Scattering and Emission Models and Their Applications. Norwood, MA: Artech House

Ferrazzoli P and Guerriero L. 1996. Passive microwave remote sensing of forests: a model investigation. *IEEE Transactions on Geoscience and Remote Sensing*, **34**: 433—443

Ferrazzoli P, Guerriero L and Wigneron J P. 2002. Simulating L-band emission of forests in view of future satellite applications. *IEEE Transactions on Geoscience and Remote Sensing*, **40**(12): 2700—2708

Jackson T J and Schmugge T J. 1991. Vegetation effects on the microwave emission from soils. *Remote Sensing of Environment*, **36**: 203—210

Karam M and Fung A K. 1988. Electromegnatic wave scattering from some vegetation samples. *IEEE Transactions on Geoscience and Remote Sensing*, **26**(6): 799—808

Karam M. 1997. A physical model for microwave radiometry of vegetation. *IEEE Transactions on Geoscience and Remote Sensing*, **35**(4): 1045—1058

Lang R, Utku C and O'Neill P. 2004. Role of albedo in assessing soil moisture under vegetation with passive L-band algorithms. Proc. of IGARSS'04 . Anchorage, Alaska, USA

Le Vine D M, Meneghini R and Lang R H. 1983. Scattering from arbitrarily orientated dielectric disks in the physical optics regime. *Journal of the Optical Society of America*, **73**:1255—1262

Njoku E G, and Jackson T G. 2003. Soil moisture retrieval from AMSR-E. *IEEE Transactions on Geoscience and Remote Sensing*, **41**(2): 215—229

RPG-8CH-DP user manual, Radiometer Physics GmbH Co. http://www.radiometer-physics.com.. (2008-11-25)

Ulaby F T, Moore R K and Fung A K. 1986. Microwave Remote Sensing: Active and Passive,Vol.3. Dedham, MA: Artech House

Vecchia A D, Ferrazzoli P and Guerriero L. 2004. Modeling microwave scattering from long curved leaves. *Waves in Random Media*, **14**(2): S333—S343(1)

Zhang Z J, Zhang L X and Zhao S J. 2008. The technical report of microwave scattering and attenuation characteristics of typical crop. Beijing:Beijing Normal University

附中文参考文献

张钟军，张立新，赵少杰. 2008. 典型作物的微波散射和衰减特性技术报告. 北京：北京师范大学